Snow and the ground temperature record of climate change

Marshall G. Bartlett, David S. Chapman, and Robert N. Harris
Department of Geology and Geophysics, University of Utah, Salt Lake City, Utah, USA

Received 12 August 2004; revised 15 September 2004; accepted 6 October 2004; published 11 December 2004.

[1] Borehole temperature-depth profiles contain a record of surface ground temperature (SGT) changes with time and complement surface air temperature (SAT) analysis to infer climate change over multiple centuries. Ground temperatures are generally warmer than air temperatures due to solar radiation effects in the summer and the insulating effect of snow cover during the winter. The low thermal diffusivity of snow damps surface temperature variations; snow effectively acts as an insulator of the ground during the coldest part of the year. A numerical model of snow-ground thermal interactions is developed to investigate the effect of seasonal snow cover on annual ground temperatures. The model is parameterized in terms of three snow event parameters: onset time of the annual snow event, duration of the event, and depth of snow during the event. These parameters are commonly available from meteorological and remotely sensed data making the model broadly applicable. The model is validated using SAT, subsurface temperature from a depth of 10 cm, and snow depth data from the 6 years of observations at Emigrant Pass climate observatory in northwestern Utah and 217 station years of National Weather Service data from sites across North America. Measured subsurface temperature-time series are compared to changes predicted by the model. The model consistently predicts ground temperature changes that compare well with those observed. Sensitivity analysis of the model leads to a nonlinear relationship between the three snow event parameters (onset, duration, and depth of the annual snow event) and the influence snow has on mean annual SGT. *INDEX TERMS:* 1645 Global Change: Solid Earth; 1694 Global Change: Instruments and techniques; 3344 Meteorology and Atmospheric Dynamics: Paleoclimatology; 1863 Hydrology: Snow and ice (1827); 3322 Meteorology and Atmospheric Dynamics: Land/atmosphere interactions; *KEYWORDS:* snow cover, ground temperatures, climate change, snow modeling, land/atmosphere interactions, borehole climate reconstructions

Citation: Bartlett, M. G., D. S. Chapman, and R. N. Harris (2004), Snow and the ground temperature record of climate change, *J. Geophys. Res.*, *109*, F04008, doi:10.1029/2004JF000224.

1. Introduction

[2] To improve our understanding of climate variations in recent centuries it is desirable to extend estimates of surface air temperatures (SAT) beyond the approximately 150 years of available instrumental data. Borehole temperature-depth profiles offer one promising technique for reconstructing surface ground temperatures (SGT) prior to available meteorological records [*Lachenbruch and Marshall*, 1986; *Pollack and Chapman*, 1993; *Harris and Chapman*, 1995, 2001; *Pollack and Huang*, 2000]. In thermally conductive subsurface environments, variations in SGT propagate downward at rates governed by the thermal diffusivity of the ground. Perturbations to the background thermal regime are manifest at depths in the Earth that are characteristic of the timing of the surface temperature change. For typical crustal values of thermal diffusivity (1×10^{-6} m^2 s^{-1}), step changes in temperature that took place 100 and 1000 years ago would be manifest as a perturbation extending to depths of about 100 and 300 m, respectively. By measuring temperatures in boreholes of appropriate depth, the history of SGT variations can be reconstructed.

[3] SGT histories from a global compilation of borehole temperature-depth measurements indicate approximately 1.0 K of surface warming over the past 500 years [*Huang et al.*, 2000; *Harris and Chapman*, 2001; *Beltrami*, 2002]. Global records of SAT variation indicate warming of approximately 0.65 K over the past 150 years [*Jones et al.*, 2000]. *Harris and Chapman* [2001] quantitatively demonstrated that variations in SATs and the transient part of temperature-depth profiles are in good agreement over the common period of overlap. This relationship indicates that air and ground temperatures are well coupled over centennial timescales and that SGT histories can be combined with SAT records to extend the history of surface temperature variations back in time. However, the energy exchange at the air-ground interface is complicated and a better understanding of the processes governing the exchange of energy across this interface at multiple timescales would improve our understanding of the relationship between air and ground temperatures.

0148-0227/04/2004JF000224

[4] One measure of the energy exchange across the air-ground interface is the difference between air and ground temperatures. If the difference is constant at decadal and longer timescales, then climate change inferred from either SAT analysis or SGT (borehole) analysis should be the same. If the air and ground temperature difference changes with time SAT and SGT analyses could produce contradictory inferences of climate change. Factors that may affect the air-ground temperature difference include annual snow cover, precipitation, solar insulation, land use changes including deforestation, and a variety of microclimatic and biological interactions. At midlatitudes, the difference is largely governed by the differential absorption of solar energy during summer months causing ground temperatures to be warmer than air temperatures [*Powell et al.*, 1988; *Putnam and Chapman*, 1996]. During the winter when snow is present, the difference between ground and air temperatures is more complicated. Understanding these boundary interactions and their relationship to the difference between air and ground temperatures through time is critical to understanding the coupling between SAT and SGT at multiple timescales.

[5] This study investigates the influence of annual snow cover on differences between mean annual and mean seasonal SAT and SGT. Snow influences the coupling between SAT and SGT by adding a low thermal diffusivity layer between the air-ground interface during the coldest part of the year, effectively insulating the ground and muting its response to extreme air temperatures. We develop a snow-ground thermal model to explore how these factors, in combination with changing timing and duration of snow cover, influence ground temperatures; the model is validated and applied to data from U.S. National Weather Service (NWS) Co-Op sites and from Emigrant Pass Observatory (EPO) in northwestern Utah where we have collected detailed data on the air-ground interface since 1993.

[6] We emphasize at the outset that our focus is on how snow effects ground temperatures. This emphasis is different than that found in most snow models in which the evolution of the state variables of the snow pack are modeled at fine temporal scales; generally such models are more concerned with understanding water storage in snow or in anticipating runoff from a snow pack and require much larger numbers of input parameters than are available from meteorological field sites. In addition, many of the current state-of-the-art snow models include only coarse representations of the underlying ground thermal regime [*Essery and Yang*, 2001]. Our focus on understanding the ground's thermal state beneath a snow pack at seasonal to annual timescales and over broad spatial regions requires a different approach.

[7] We use a one-dimensional, two layer finite difference model of snow-ground thermal interactions to quantify the sensitivity of the ground's thermal response to three snow event parameters: maximum snow depth, snow event onset time, and snow event duration. These parameters are commonly available from meteorological or satellite data; namely, SAT, snow onset, duration, and snow depth. While our approach neglects some details of the physical processes operating for limited lengths of time within the snow pack (snow melt dynamics, percolation of water through the snow pack, snow stratification, etc.), comparisons of model output with measured SAT and ground temperatures at a variety of locations in North America suggest that a relatively simple model is capable of capturing the first-order thermal effects snow has on ground temperatures at longer timescales (seasonal to annual). We start by developing the snow-ground thermal model and investigating its sensitivity to snow event parameters. We then give a brief outline of the data sets used to validate the model, including data from Emigrant Pass Observatory. We conclude by validating our model using air and ground temperature data from EPO and a set of NWS Co-Op sites.

2. Snow-Ground Thermal Model

[8] *Goodrich* [1982] demonstrated that snow-ground thermal interactions can be effectively modeled using a one-dimensional finite difference approximation of the heat equation for a two-layer composite medium consisting of an insulating layer (snow) lying over an infinite half-space of porous, partially saturated rock. We adopt a similar approach here, updated with several advances made since the original Goodrich study. We use a forward finite difference scheme to approximate the solution to the apparent heat capacity formulation of the heat equation. We include latent heat absorption and release in the ground layer of the model via an apparent heat capacity formulation of the heat equation in this layer. Though latent heat exchange in the ground should have no influence on mean annual SGT in temperate locations (the same amount of heat is released as ground freezes in the fall as is absorbed as the ground thaws in the spring), it can have a significant seasonal influence on SGT.

[9] Conductive heat transport through the shallow ground thermal regime responds to temperature changes at the surface and satisfies

$$C^A(T)\frac{\partial T}{\partial t} = \frac{\partial}{\partial z}\left(k\frac{\partial T}{\partial z}\right), \tag{1}$$

where $C^A(T)$ is apparent volumetric heat capacity as a function of temperature, T, t is time, z is depth, and k is thermal conductivity. Following *Yao and Chait* [1993], we use a homographic approximation for the function $C^A(T)$ in (1) given by

$$C^A(T) = c\rho + L\rho\frac{\partial f(T)}{\partial T}, \tag{2}$$

where the product of the specific heat, c, and material density, ρ, is the volumetric heat capacity, C, L is latent heat, and $f(T)$ is the homographic function developed by *Yao and Chait* [1993]. This approach has the advantage of spreading the thermal effects of latent heat exchange at the phase transition over a broader temperature region than a Heaviside function, reducing the possibility of missing the latent heat effect under rapidly changing boundary conditions.

[10] We convert (1) into a finite difference equation,

$$C^A\left(T_j^n\right)\frac{T_j^{n+1} - T_j^n}{\Delta t} = k_j\frac{\left(T_{j+1}^n - 2T_j^n + T_{j-1}^n\right)}{(\Delta z)^2}, \tag{3}$$

Table 1. Stefan-Neumann Problem Parameters

Model Parameter	Symbol	Units	Frozen[a]	Unfrozen[a]
Thermal conductivity	K	W m^{-1} K^{-1}	2.2	0.60
Density	ρ	kg m^{-3}	917	1000
Specific heat	C	J kg^{-1} K^{-1}	3400	4182
Diffusivity	α	m^2 s^{-1}	7.1×10^{-7}	1.4×10^{-7}
Latent heat	L	J kg^{-1}	3.3×10^5	N/A

[a]Values are those for water, as detailed in the text.

and solve for T_j^{n+1} at the $n + 1$ time node:

$$T_j^{n+1} = \frac{k_j}{C^A\left(T_j^n\right)} \Delta t \frac{\left(T_{j+1}^n - 2T_j^n + T_{j-1}^n\right)}{(\Delta z)^2} + T_j^n. \quad (4)$$

[11] This solution is stable when the temporal and spatial step sizes in each model layer do not violate the inequality

$$2\Delta t\left(\frac{k}{C^A}\right) < (\Delta z)^2. \quad (5)$$

[12] Temperature continuity is maintained between the two layers by equating the temperatures at the layer interface. Values of Δt and Δz used in this study are 180 s and 0.05 m, respectively, and satisfy inequality (5). For our application with a distinct contrast in thermal parameters between the ground and snow, this forward explicit method has the advantage of maintaining accuracy in the region of sharp parameter contrasts [*Press et al.*, 1992].

[13] The upper boundary of the model, either the ground surface when no snow is present or the snow surface when snow is present, is set by prescribing temperature at all temporal nodes corresponding to the surface temperature driving function. The model domain extends 10 m into the ground layer where the annual variation in heat flow is less than 5% of the surface variations and has negligible effect on near surface temperatures on an annual timescale. Consequently, it is adequate to represent the lower boundary with a constant geothermal heat flow value at this depth. For our sensitivity tests the initial condition for all depth nodes is specified by running the model for a year in which all nodes start at the mean of the annual temperature and during which no snow is present. When the model is applied to actual data sets in which a previous years observations are available, the initial condition is set by running the model with the previous year's measured parameters.

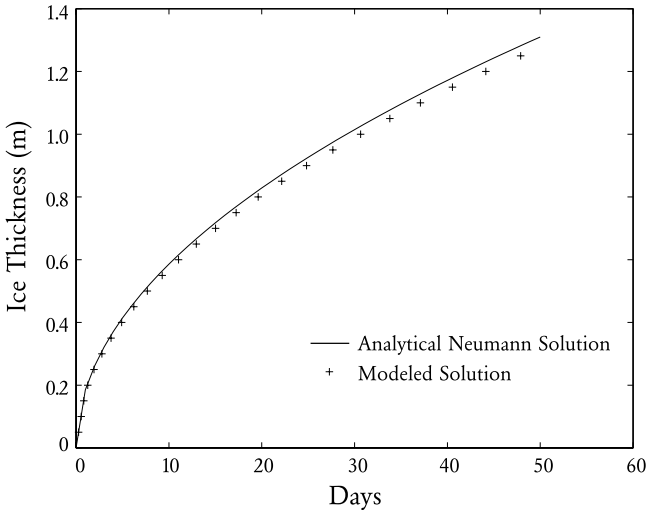

Figure 1. Stefan-Neumann freezing solutions. Solution values indicate the time step in the model at which each node passes through the phase change temperature. The modeled solution departs slightly from the analytic solution at larger time values due primarily to the approximation of latent heat contributions. However, the model clearly is a valid approximation of heat conduction in a regime with phase transition.

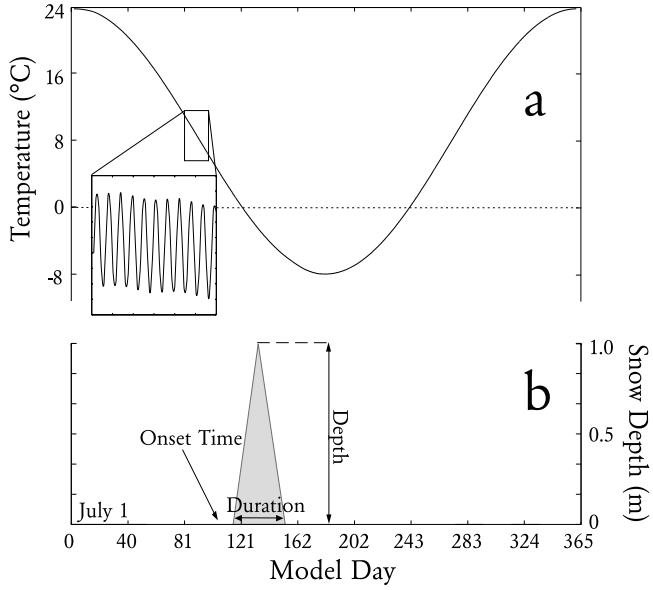

Figure 2. The snow-ground thermal model input (a) surface air temperature time series and (b) snow event. The temperature fluctuations are based on daily and annual variations at Emigrant Pass Observatory. The diurnal variations are shown at an expanded timescale for clarity (box). The snow event is shown as shaded region and is parameterized in terms of onset time, duration, and maximum snow depth.

[14] To verify both the conductive and latent heat aspects of the model, we apply the model to a two phase Stefan freezing problem following the example of *Goodrich* [1978]. Four characteristics make the Stefan problem an appropriate test of our model's characteristics: it is purely conductive, it is two layered, it incorporates the effects of latent heat exchange, and it has an analytic solution. Additionally, using the thermal parameters of a media such as water with a relatively high latent heat emphasizes the energy exchange at the phase boundary, making this case an extreme test of the model's ability to handle latent heat effects. We consider a homogenous half-space of material at some constant initial temperature, $T_i = 2°C$, greater than the temperature of the phase change, $T_p = 0°C$. For all times, $t > 0$, the temperature at the upper boundary, $T_u = -10°C$, is set to a value below the phase change. As time advances, a frozen layer forms at $z = 0$ and begins

Table 2. Summary of Surface Air Temperature (SAT) and Ground Temperature Observations From Emigrant Pass Observatory (EPO), 1993–2001

Observation Period	Maximum SAT, °C	Minimum SAT, °C	Mean SAT, °C	Mean GT,[a] °C	GT-SAT, °C	Estimated Error, °C
DJF	13.50	−17.61	−2.32	−2.41	−0.09	0.10
MAM	29.14	−10.53	8.80	11.17	2.37	0.00
JJA	36.87	0.51	22.11	26.10	3.99	0.00
SON	33.62	−17.37	7.94	11.32	3.38	0.02
Dec. 1993–1994	36.87	−17.61	9.13	11.54	2.41	0.03
DJF	16.35	−18.13	−0.77	−0.49	0.28	0.30
MAM	23.29	−8.56	5.45	8.07	2.62	0.02
JJA	35.54	−1.14	19.04	22.77	3.73	0.03
SON	33.72	13.04	9.20	10.81	1.61	0.15
Dec. 1994–1995	35.54	−18.13	8.23	10.29	2.06	0.13
DJF	16.03	−21.44	−1.94	−0.83	1.11	0.05
MAM	28.13	−7.98	7.12	10.13	3.01	0.17
JJA	36.95	3.94	22.05	24.87	2.82	0.04
SON	31.14	−8.01	12.00	16.95	4.95	0.22
Dec. 1995–1996	36.95	−21.44	9.81	12.78	2.97	0.12
DJF	BF[b]	BF	BF	BF	BF	BF
MAM	30.48	−8.76	8.20	11.20	3.00	0.12
JJA	34.54	4.29	19.69	23.96	4.27	0.05
SON	30.87	−12.32	8.07	12.98	4.91	0.06
Dec. 1996–1997	BF	BF	BF	BF	BF	BF
DJF	9.82	−16.40	−2.12	−2.39	−0.27	0.25
MAM	24.30	−14.52	5.83	8.12	2.29	0.12
JJA	38.41	0.00	19.96	23.98	4.02	0.06
SON	33.74	−7.22	8.58	12.91	4.33	0.18
Dec. 1997–1998	38.41	−16.40	8.06	10.66	2.59	0.15
DJF	13.69	−22.23	−2.15	−1.58	0.57	0.18
MAM	28.28	−8.72	5.84	9.14	3.30	0.09
JJA	35.38	−0.10	20.42	24.21	3.79	0.21
SON	30.55	−11.03	7.73	13.26	5.53	0.20
Dec. 1998–1999	35.38	−22.23	7.96	11.26	3.30	0.17
DJF	11.25	−19.73	−1.11	−0.62	0.49	0.40
MAM	27.33	−6.22	6.48	9.39	2.91	0.11
JJA	34.41	4.17	20.35	23.86	3.51	0.30
SON	32.67	−5.89	13.84	19.00	5.16	2.30
Dec. 1999–2000	34.41	−19.73	9.89	12.91	3.02	0.78
DJF	10.72	−15.22	−3.09	−1.81	1.28	2.40
MAM	32.45	−8.18	8.78	14.19	5.41	0.25
JJA	39.08	0.21	22.09	26.35	4.26	0.00
SON	33.38	−5.66	13.19	18.74	5.55	0.30
Dec. 2000–2001	39.08	−15.22	10.24	14.37	4.13	0.74

[a]GT, ground temperature measured at a depth of 10 cm.
[b]Battery failure during period.

to thicken. Values for model thermal parameters used in the Stefan-Neumann problem are given in Table 1. The model solution is compared to the analytic solution (Figure 1). Crosses indicate the time step at which the phase change passes through each node. In general the comparison is very good, although the model solution departs slightly from the analytic solution at large times. This departure is primarily due to the fact that some latent heat contributions are missed at early times due to the spatial and temporal discretization.

3. Sensitivity Tests

[15] Using the snow-ground thermal model, we perform a number of sensitivity tests to investigate the influence of snow events on differences between air and ground temperatures. For these tests we idealize the temperature-time series in terms of two superimposed cosine waves, one with period of 1 year representing the annual cycle and another with a period of 1 day representing diurnal temperature variations (Figure 2a). Note that these idealized cosine waves are only used in our sensitivity studies; in application of the model to real data sets observed values of temperature are used as model input. Values of the amplitude for both annual and diurnal variations and the mean of the annual cycle in these calculations are based on the meteorological observations at EPO (Table 2) and are representative of a broad range of locations in midlatitudes. For our sensitivity studies synthetic snow events are generated which consist of a linear accumulation to the event's maximum depth followed by a linear ablation to produce a triangular shape (Figure 2b). As with the idealized temperature-time series, in application of the model to real data observed values of the snow depth as a function of time are employed. We investigate the importance of snow event shape by also testing boxcar shaped events in which all the snow appears in a single time step, maintains a constant thickness, and disappears in a single time step. These two end member cases indicate that the sensitivity of the SGT to the shape of the snow event is small relative to the influence of other parameters. This result is consistent with the extremely low thermal diffusivity of the snow layer; even a small amount of snow is sufficient to insulate the ground from sensing diurnal variations in surface air temperature.

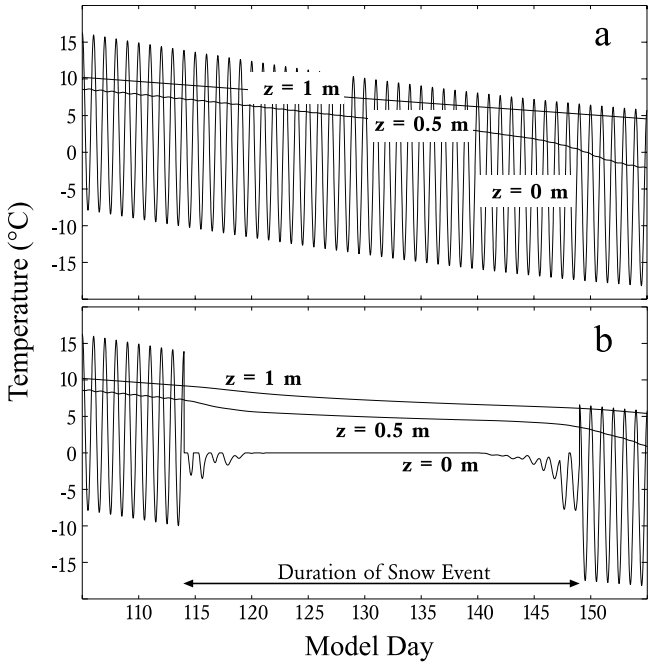

Figure 3. Snow-ground thermal model output. (a) Model output in the absence of a snow event. (b) Model output for a snow event with onset at day 114 and a duration of 35 days (the event in Figure 2). We show temperatures as a function of time for three depths. The snow acts as a blanket, sheltering the ground surface from fluctuations at the boundary of the model. The effect is pronounced at the ground surface and attenuates at greater depths.

[16] In the example illustrated in Figure 2, the onset time at model day 114 (23 October) and duration (35 days) for the synthetic snow event are chosen to illustrate the effects of the phase change in the subsurface. Snow starts to accumulate while the daily mean temperature is +4°C with highs and lows of 14°C and −6°C, respectively. When the snow event reaches its maximum depth, daily mean temperature has dropped to −6°C with daily maximum and minimum temperatures of 4°C and −16°C, respectively. To simplify the discussion, we neglect the difference between SAT and SGT due to absorbed radiation. This simplification allows us to equate SGT and SAT in the absence of snow. This is a reasonable first-order simplification because solar radiation has its strongest effect in the summer [*Putnam and Chapman*, 1996]. The contrast in ground temperature response at 0 m due to ignoring the snow event versus incorporating the snow event are illustrated (Figures 3a and 3b, respectively) at an expanded timescale to show the details of heat propagation. The ground temperature is shown at three depths to demonstrate the effect of diffusion in the ground's response to the model's surface driving function. For the snow free case, the $z = 0$ depth node (Figure 3a), is simply the model's surface driving function which in this case is the synthetic SAT time series (Figure 2a). Temperatures at $z = 0.5$ m and $z = 1.0$ m illustrate the attenuation and phase lag associated with conductive media. At 0.5 m depth, diurnal variations are visibly damped and phase shifted, and at 1 m depth diurnal variations are negligible. Mean temperatures for these two depths during the illustrated period are warmer than mean surface temperatures due to the lag associated with the previous summer's warmer temperature. Note also the reduction in temperatures at $z = 0.5$ in late November. This temperature drop is due to the effect of latent heat. Prior to this time the temperature is maintained close to 0°C while the ground freezes; the relatively abrupt temperature drop indicates that the phase change is complete at this depth.

[17] With the onset of snow and increasing snow thickness, variations in the SAT driving function are increasingly attenuated, both because of the increasing snow thickness, and the low thermal diffusivity of snow relative to ground (Figure 3b). The ground surface ($z = 0$ m) experiences a damped and lagged version of the temperatures at the snow surface. The net effect of the snow event is to raise the annual mean SGT from 8° to 8.15°C relative to the snow free case. At 0.5 m, the ground is warmed from 6.82° to 7.02°C and at 1 m depth the ground warms from 7.66° to 7.83°C. This example illustrates that even a relatively short-duration snow event can produce a discernible offset in mean annual SGT as well as on temperatures measured at shallow depths within the ground.

[18] To investigate the influence of the maximum snow depth on the average annual ground surface temperature, we fix the duration and onset time of the snow event in our model, and run the model multiple times with different maximum depths of the snow event in each model run. The difference is then taken of the annual mean SGT (at $z = 0$ m in the ground layer) with the snow event and the annual

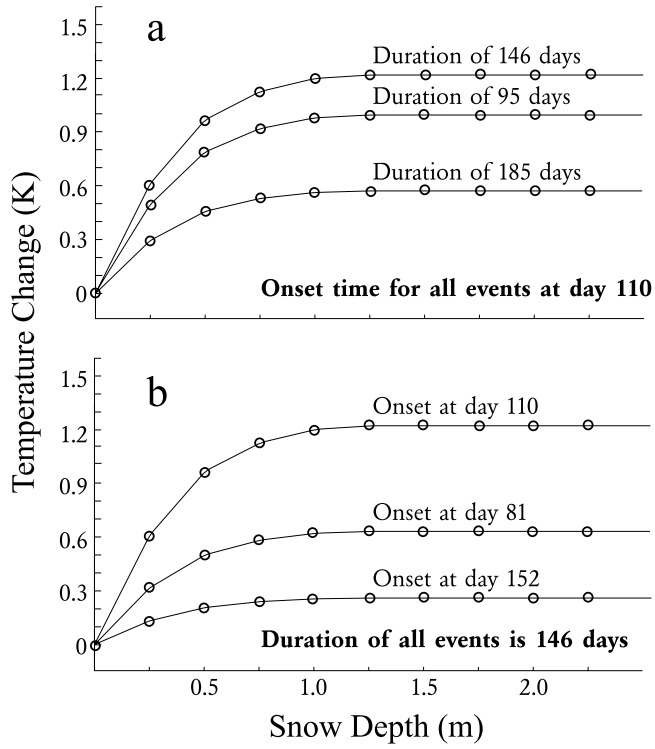

Figure 4. Annual air-ground temperature difference as a function of snow depth with changing (a) duration and (b) onset time. After a critical thickness (∼1 m) of snow is reached, increasing snow thickness to values greater than 1 m does not affect the annual surface ground temperature.

mean SGT with no snow present. The value calculated in this way is the influence snow has on mean annual ground temperatures, i.e., the "snow effect."

[19] The results of this modeling for three different variations of onset time and three variations of duration are illustrated in Figure 4. These onset and duration parameters are chosen to bracket the largest possible warming from snow events in northwestern Utah (discussed later). Two interesting features are illustrated. First, snow events have the effect of changing the annual mean SGT monotonically for snow thicknesses from 0 to 1 m with little additional influence for thicknesses beyond 1 m. Secondly, the magnitude of the influence varies with the onset time and duration of the event.

[20] After the snow reaches a critical thickness of about 1 m, additional increases in thickness result in no discernable influence on the mean SGT. Essentially, 1 m of snow is sufficient insulation to damp all surface fluctuations with periods less than several months from reaching the ground. This critical thickness of 1 m is remarkably stable with respect to variations in the duration and onset time of the event (Figure 4). This critical thickness value is a function of the snow thermal parameters. Altering these parameters changes the efficiency with which the snow insulates the ground surface, effectively changing the critical thickness of snow.

[21] That some critical thickness of snow should exist can be demonstrated and its approximate value calculated from a simple investigation of the skin depth of snow cover. Recall that for some periodic surface fluctuation conducted into a media skin depth, l, is defined as

$$l = \sqrt{\frac{2\alpha}{\omega}}, \tag{6}$$

where α is the thermal diffusivity and ω is the frequency of the surface variation. The skin depth specifies the depth at which the surface fluctuation amplitude is damped to a value of 1/e of its value at the surface. For snow cover with a diffusivity on the order of $\alpha = 1 \times 10^{-7}$ m^2 s^{-1} and a diurnal surface fluctuation ($\omega = 1.16 \times 10^{-5}$ s^{-1}) the skin depth is a mere 0.1 m. For an annual cycle ($\omega = 3.1 \times 10^{-8}$ s^{-1}), the skin depth of the snow cover is 1.7 m. Thus surface fluctuations with periods shorter than that of the annual cycle are effectively damped prior to reaching the ground surface by the presence of even a small amount of snow cover.

[22] The second feature shown in Figure 4 is that the magnitude of the snow effect on ground temperature varies with the onset time and duration of snow cover. Conceptually, if snow covers the ground when the SAT curve is above 0°C, the ground will be cool relative to the case of no snow cover; that is, the snow insulates the ground from the warm air temperatures. If snow covers the ground when SAT curve is below 0°C, the ground will remain relatively warm; that is, the snow insulates the ground from the cold air temperatures. The magnitude of the snow effect on ground temperature is a strong function of the SAT curve.

[23] Maximum warming of the ground for the SAT driving function used in these sensitivity tests (and illustrated in Figure 2) occurs at an onset time around 19 October with duration of 146 days (an event that lasts from 19 October until 14 March). This corresponds to snow coming just before the SAT curve cools through the 0°C isotherm and disappears just after the SAT curve warms through the 0°C isotherm. For snow events that begin on 19 October, shorter-duration events have a lesser effect on changing the mean annual SGT because the ground is insulated from fewer days of below freezing winter temperatures (Figure 4a). Longer duration events also have less of a warming influence since the insulation during winter days is being negated by snow remaining into the spring when average daily temperatures are above 0°C. Altering the onset of the snow event in either direction from 19 October while holding the duration of the snow event fixed results in a reduction of ground warming because the period of time for which the ground is decoupled shifts away from when air temperatures are below 0°C to times when they are above freezing (Figure 4b).

[24] Sensitivity of the mean annual SGT as a function of snow event onset and duration for snow thicknesses with a maximum of 1.0 m is illustrated in Figure 5. Simulations are calculated across a grid of 10,000 snow events (100 × 100) with constant spacing in both onset time and duration across a model year. Contours show the difference between the mean annual SGT with snow and the mean annual SAT (SGT without snow). Snow events with an onset near the end of a model year and a duration extending into the next year are accommodated by running three consecutive years with the onset occurring in the second year.

[25] The overall shape and magnitudes of the contours are also sensitive to the mean annual SAT curve, and it is the complex interplay between SAT and the presence or absence of snow that dictates the difference between SAT and SGT. The presence of snow cover can therefore cause both positive (ground warming) and negative (ground cooling) temperature differences. For example, the maximum annual warming of the ground is on the order of 1 K, corresponding to snow events that cover the ground during the period of time for which the SAT is less than 0°C (November to March). The 1 K magnitude of ground warming is the difference between the mean annual SAT (mean annual SGT without snow) and the mean annual SGT with snow. Simply put, the snow is insulating the ground from cold air masses. In contrast, for this example the maximum annual cooling of the ground is on the order of 8 K, corresponding to snow events that cover the ground surface for period of time for which the SAT is above 0°C. The mean annual SAT for this example is 8°C while the snow event effectively holds the SGT at 0°C, resulting in a temperature difference of −8 K. In this case the snow is insulating the ground from warm air masses. While this is physically unreasonable on annual timescales (snow cover coming late in the winter or spring and lasting through the summer), minor cooling of the ground can still occur if heavy snow cover comes late in the winter and lasts through much of the spring.

[26] In addition to the annual warming and cooling events illustrated in Figure 5, there is also the possibility that a snow event can have little influence on the mean annual SGT (events that fall near the 0 K contour line). These events are usually centered on the transition of the SAT from mean daily temperatures that are above zero to mean daily temperatures that are below zero and vice versa. If the

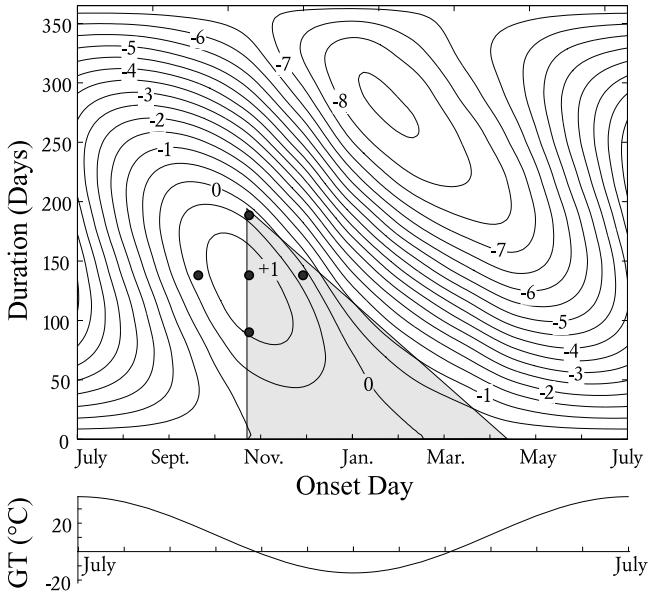

Figure 5. Influence of snow event onset time and duration on annual surface ground temperatures. Contours illustrate the difference in °C between the average annual surface ground temperature with a snow event and the model driving function (labeled GT here). Filled circles indicate the locations of model runs illustrated in Figure 4. The triangular shaded area is the limits of the parameter space observed at EPO and nearby National Weather Service (NWS) stations in northwestern Utah. The lower plot shows the annual driving function (SAT).

snow event is such that it clips equal amounts of net ground cooling and net ground warming, it is possible that it will leave no discernable signal in the mean annual ground surface temperature. Long-term (decadal to centennial) changes in snow seasonality also may have little net effect on the offset between SGT and SAT if longer duration snow events are accompanied by earlier snow onsets or short-duration events are accompanied by later onsets (effectively moving subparallel to contour lines in Figure 5). Alternatively, annual snow events evolving toward earlier onset times and shorter durations, or later onset times and longer durations, could produce substantial changes in the offset between air and ground temperatures.

[27] The shaded area in Figure 5 encompasses the conditions observed in northwestern Utah based on National Weather Service records over the past 100 years and is included to illustrate the range of the parameter space observed at EPO (see next section). Snow seldom accumulates before 21 October and has generally disappeared by 7 April. Thus maximum warming and cooling of ground temperatures due to snow within this shaded area are a little greater than +1 K and −1 K, respectively for a snow thickness of 1 m.

4. Data Used for Model Verification

[28] An important component of this study involves validating the snow-ground thermal model using observed data. Two data sets are used for this validation. The first data set comes from our climate observatory in northwestern Utah. Understanding the coupling of air and ground temperatures at this site provided the original motivation for the construction of the snow-ground thermal model. Since the site in northwestern Utah was located to minimize many of the complicating factors in air-ground coupling, we also extend our verification test to a set of National Weather Service Co-Op stations from five states in the continental United States.

4.1. Emigrant Pass Observatory, Northwestern Utah

[29] Emigrant Pass Observatory (41°30′N, 113°42′W, elevation 1750 m) is located on the southeastern flank of the Grouse Creek Mountains in northwestern Utah, along the eastern edge of the Basin and Range physiographic province. Situated on exposed granitic rock, EPO consists of a standard meteorological observatory installed next to a 150 m deep borehole, GC-1 (Figure 6). Instrumentation at EPO consists of a solar powered Campbell Scientific CR-10 data logger controlling a suite of meteorological instruments and two sets of shallow (1 m) thermistor strings used to measure ground temperatures. The EPO meteorological array includes measurements of air temperature, relative humidity, incoming solar radiation, precipitation, wind speed and direction, and snow depth. Specifics of instrumentation, calibration, and other aspects of the observatory at EPO are detailed by *Putnam and Chapman* [1996].

[30] The critical data in modeling and validating the snow-ground thermal model are air temperature, ground temperature, and snow depth as a function of time. Air temperatures are measured at a mast height of 2 m with a sample rate of 60 s. A mean value for each 30 min period is stored in memory. Ground temperatures are measured at depths of 2.5, 10, 20, 50, and 100 cm and are also sampled every 60 s with a mean value for each 30 min period stored in memory. Snow depth is sampled every 30 min and the maximum value for each 24 hour period is stored in memory. Thus each 24 hour period consists of 48 measurements for each air and ground thermistor and a single value for mean snow depth.

[31] The range of air and ground temperatures observed at EPO between December 1993 and December 2001 are reported in Table 2. The data are broken into standard 3 month meteorological seasons (DJF, MAM, JJA, and SON). This partitioning allows us to separate seasonal signals within the annual means such as solar radiative heating of the ground surface during the summer [*Putnam and Chapman*, 1996].

[32] Air temperatures at EPO range from 39°C to −22°C (Table 2). The annual mean SAT at the site varies between 10.24°C and 7.96°C. Maximum annual temperatures range from 39.08°C to 34.41°C, while minimum temperatures range from −21.44°C to −15.22°C. Mean annual ground temperatures at a depth of 10 cm range from 14.37°C to 10.29°C. Ground temperatures have magnitudes in the summer months as much as 5 K warmer than SAT values for the same period due to incident solar radiation. When ground temperatures are compared with SAT values at EPO, they show phase lag, diminished peak-to-peak amplitude, and frequency attenuation consistent with a conductive thermal regime. Furthermore, decadal changes in subsurface temperature track decadal changes in SAT records from

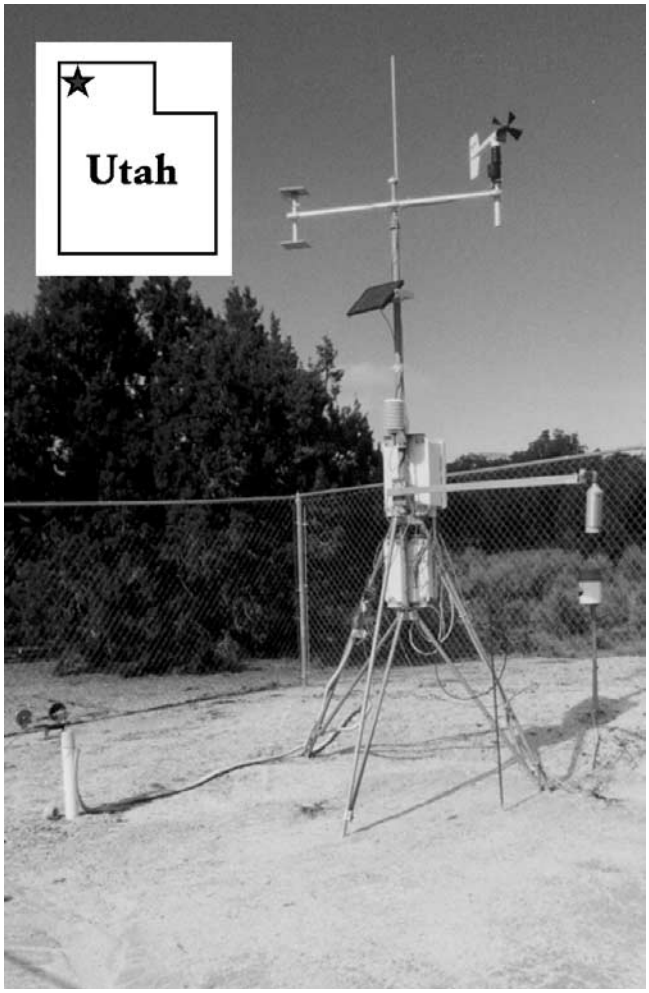

Figure 6. EPO, northwestern Utah, USA. Inset shows location of EPO. Meteorological instruments include temperature sensors (center), solar radiation (upper left), wind speed and direction (upper right), and an acoustic snow depth gauge (far right). The borehole (GC-1) is visible in the lower left (white PVC pipe).

nearby meteorological stations indicating that heat transfer in the subsurface is dominated by conduction [*Chapman and Harris*, 1993].

[33] Two sources of error influence the numbers in Table 2, the precision of the ground thermistors and the distribution of sensor failures and missing data. Thermistor precision is 5 mK providing a lower bound to the error estimates for ground temperatures [*Putnam and Chapman*, 1996]. We estimate the error associated with missing data points by utilizing the first year, in which no data were lost. From this year we remove an arbitrary period of data and refill the gap using an augmented nearest-neighbor interpolation algorithm [*Bartlett*, 2001]. Seasonal means between the original and interpolated data are then compared. This process is repeated using different time sections and the statistics of the error are calculated. After repeating this procedure numerous times for different lengths of interpolation, we arrived at a mean error associated with each length of data gap. The expected error in the seasonal mean for the interpolation of a single missing data point (one 30 min reading) is less than 1×10^{-6} K with a standard deviation of less than 1×10^{-3} K. For a section of missing data 150 points long (slightly more than 3 days of missing data) the expected error of any single point within the interpolation is about 6×10^{-6} K with a standard deviation of 5×10^{-3} K. Final errors are assigned to seasonal and annual means in Table 2 by summing the expected error and two standard deviations of each missing point over all the missing data. Reported errors indicate a 95% confidence interval for the reported mean.

[34] Table 3 summarizes the snow data at EPO. Recorded snow events range from winters during which no snow was recorded at the site (1993–1994, 1999–2000) to winters during which snow was present in excess of 112 days. Snow events during 1996–1997 were only partially recorded due to battery failure of the station that year. A problem with the snow sensor caused data loss during the 1997–1998 and 2000–2001 snow seasons. The three available snow seasons from EPO are illustrated in Figure 7. The 1994–1995 season (event A) begins in the late fall and lasts until early spring. The 1995–1996 and 1998–1999 seasons (events B and C, respectively) do not begin until midwinter and last until early spring. The maximum snow depth of event C is only about 0.15 m compared to nearly 0.30 m for both events A and B. Accumulation patterns also vary from year to year; event A shows a gradual accumulation to the maximum snow depth followed by a rapid ablation of snow, while event B shows a rapid build up, followed by a more gradual ablation.

4.2. NWS Co-Op Stations

[35] In addition to the data from EPO, we apply the snow-ground thermal model to data from 23 National Weather

Table 3. Snow Data From EPO

Snow Year	Event Label	Snow Onset	Duration, days	Maximum Depth, cm
June 1993–1994		...	0	0.0
June 1994–1995	A	2 Nov. 1994	112	29.7
June 1995–1996	B	16 Jan. 1996	60	33.6
June 1996–1997		BF[a]	BF	BF
June 1997–1998		SF[b]	SF	SF
June 1998–1999	C	20 Jan. 1999	42	14.6
June 1999–2000		...	0	0.0
June 2000–2001		SF	SF	SF

[a]BF, battery failure.
[b]SF, snow sensor failure.

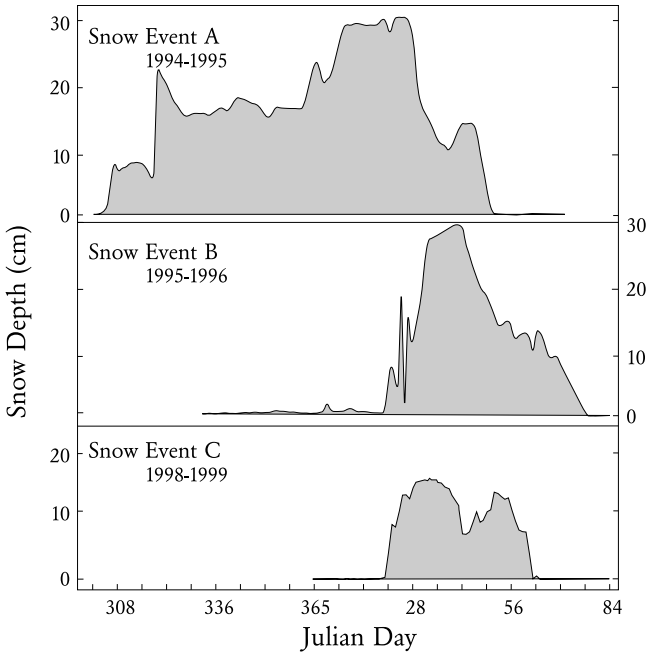

Figure 7. Snow events at EPO. Dates are given in calendar months; each tick on the time axis represents 1 week. Events are labeled A, B, and C. Information about each event is given in Table 3.

Service Co-Op stations located in five states (Alaska, Utah, Idaho, New York, and Maine); 217 station years with ground temperature observations are available from these sites. Station identification numbers and locations (latitude and longitude and elevation) for the NWS stations used in this study as well as the years of data used from each station are given in Table 4. Observations at each site include maximum and minimum daily air temperature, daily snow depth, and maximum and minimum daily ground temperature observed at 10 cm depth. Locations were chosen to represent a diversity of ground surface conditions (ranging from bare soil to tall grass cover), a diversity of soil types (coarse grained sands to loamy soils) and a wide range of seasonal snow and surface air temperature conditions. Years of record within the data set range from 1982 through 2003 with annual snow cover lasting less than a week to as long as 210 days. Thermal parameters for the snow and soil at each site are not available; instead, values representative of typical soils and snow packs are used in this study. The same thermal parameters are used for all NWS sites while a separate set of ground parameters representative of granite is used in modeling EPO (Table 5).

5. Model Verification

5.1. Emigrant Pass Observatory, Northwestern Utah

[36] We first test our model against observations of air and ground temperature collected at EPO. *Putnam and Chapman* [1996] demonstrated that a significant fraction of the difference between annual SAT and SGT at EPO is best understood in terms of solar radiation between March and November. During the summer the ground temperature may be 5 K warmer than the air temperature (Table 2), with a mean warm season temperature difference of 3.78 K. By contrast, the difference between DJF ground and air temperatures for the year in which no snow is present is remarkably small with a cold season difference of just −0.09 K. The magnitude of the annual offset at EPO from October 1993 to October 1994, a year when no snow accumulated, is approximately 2.5 K [*Putnam and Chapman*, 1996]. While radiation is the dominant cause of the difference between air and ground temperatures at the site, long-term variations in snow seasonality are more likely to affect the coupling between air and ground temperature on the timescale of decades to centuries relevant to borehole climatic studies.

[37] In order to isolate the influence of snow, from the effects of solar radiation, we examine the difference between mean observed and snow-ground thermal model predicted ground temperature for the time period when snow is on the ground. Mean observed ground temperatures

Table 4. National Weather Service (NWS) Stations Used in This Study

NWS Co-Op Station	Co-Op ID	State	Latitude, deg	Longitude, deg	Elevation, m	Years
Aberdeen Exp. Stn.	100010	ID	42:57	−112:50	1342.6	1982–1990, 1992–2003
Buhl No. 2	101220	ID	42:36	−114:45	1158.2	1998
Craigmont	102246	ID	46:14	−116:29	1143.0	1982–1983, 1987–1992, 1994–1995
Emmett 2 E	102942	ID	43:51	−116:28	728.5	1992–1993, 1995–2001
Moscow Univ. of ID	106152	ID	46:43	−116:58	810.8	1993–1996, 1998–2003
Parma Exp. Stn.	106844	ID	43:48	−116:57	698.0	1983, 1985, 1987–1995, 1997, 2002
Rexburg BYU ID	107644	ID	43:48	−111:47	1511.8	1983, 1986–1988, 1990–1991
Sandpoint Exp. Stn.	108137	ID	48:18	−116:33	640.1	1990, 1992–1993
Twin Falls 6 E	109303	ID	42:33	−114:21	1207.0	1982–1996
Caribou Munc. Airport	171175	ME	46:52	−68:02	190.2	1982–1993, 1999, 2001–2002
Canton 4 SE	301185	NY	44:35	−75:07	136.6	1982–2002
Geneva Research Farm	303184	NY	42:53	−77:02	218.8	1982–1988, 1990, 1992–1993, 2003
Ithaca Cornell Univ.	304174	NY	42:27	−76:27	292.6	1982–1993, 1996, 1998–2000, 2002–2003
Valatie 1 N	308746	NY	42:26	−73:41	91.4	1983–1988, 1990, 1997–2000, 2002
Logan SW Exp. Farm	425194	UT	41:40	−111:53	1368.6	1982, 1984–1995, 1998
Richfield Radio KSVC	427260	UT	38:46	−112:05	1615.4	1989–1991, 1994, 1996–1999, 2002–2003
St. George	427516	UT	37:06	−113:34	844.3	1989
Salt Lake International Airport	427598	UT	40:47	−111:58	1287.8	1982–1990, 1992–1994, 1996, 1999, 2001–2002
Central No. 2	501466	AK	65:34	−144:46	280.4	2002
Trapper Creek 7 SW	509398	AK	62:16	−150:25	129.5	2003
Two Rivers	509489	AK	64:52	−146:57	184.4	2002

Table 5. Snow-Ground Thermal Model Parameters

Model Parameter	Symbol	Units	Subsurface NWS[a]	Subsurface EPO[b]	Snow[c]
Thermal conductivity	K	W m^{-1} K^{-1}	0.8	2.2	0.25
Density	ρ	kg m^{-3}	1350	2750	300
Specific heat	C	J kg^{-1} K^{-1}	1000	750	2090
Latent heat[d]	L	J kg^{-1}	100,000	9900	NA
Thermal diffusivity	α	m^2 s^{-1}	5.9×10^{-7}	1.1×10^{-6}	3.9×10^{-7}

[a]Subsurface parameters are representative of sandy loams and are employed in modeling NWS site [*Abu-Hamdeh and Reeder*, 2000].
[b]Subsurface parameters are appropriate for granite and match the values used by *Putnam and Chapman* [1996].
[c]Snow parameters are representative of midlatitude snow packs [*Sturm et al.*, 1997; *Yen*, 1981].
[d]Latent heat is based on a 3% porosity of granite and the latent heat of water.

at 10 cm depth over these time periods are given in Table 6. We use observations from 10 cm depth because this thermistor gives the most reliable values and this depth is consistent with data available from the NWS sites.

[38] Figure 7 and Table 6 illustrates the range of observed snow events at EPO. The snow-ground thermal model is illustrated in Figure 8 using the early 1999 EPO snow event (event C in Table 6 and Figure 7). The upper panel illustrates the measured SAT values at the site which are used as the surface driving function in the model. The second panel is the observations of snow depth as a function of time which forms the second model input. Ground temperature observations are made at 10 cm depth in the granite and are compared in the third panel of Figure 8 to the model output ground temperatures at the same depth. The final panel highlights the differences between observed and modeled ground temperatures at 10 cm depth.

[39] Figure 8 illustrates several features of snow's influence on ground temperatures and the model's ability to simulate ground temperatures in the presence of snow. First, the presence of even a relatively small amount of snow cover is sufficient to damp high-frequency surface temperature fluctuations from entering the ground. This observation is consistent with snow having diffusivity much smaller than that of the granite at EPO. Second, the temporal evolution of the snow pack's thermal diffusivity is clearly seen in the difference between the observed and modeled ground temperatures. Since the model employs a fixed diffusivity value for the snow pack throughout the duration of the event, any alteration of the real snow's diffusivity manifests itself as an offset between the observed and modeled results. In the first half of the snow event, such an offset is clearly present; the positive value of the difference between observed and modeled ground temperatures during this period suggests that the diffusivity of the model's snow pack is too high. Freshly fallen snow would likely have a lower diffusivity than that used in the model due to greater air content prior to compaction. In mid-February, the model and the observations begin to agree much more closely. This follows a period in the SAT record of a few days of warmth followed by several days of much colder temperatures. These conditions could lead to thermally driven compaction of the snow pack, a process which would remove some of the snow's pore space, effectively altering the real snow cover's diffusivity to a value much closer to that used in the modeling. After this period, differences between the observed and modeled ground temperatures are effectively zero. The model fit for the early portion of the snow season can be improved by decreasing the thermal diffusivity from 3.9×10^{-7} to 3.5×10^{-7} m^2 s^{-1}. However by doing so, misfit in the latter portion of the snow year is increased. Because the thermal parameters of the evolving snow pack are rarely known in detail, for our analysis we have chosen a midrange value of thermal diffusivity representative of the majority of observations of seasonal snow cover [*Sturm et al.*, 1997].

[40] Finally, the role of radiative heating of the ground surface as a warm season phenomenon is illustrated by a comparison of the difference between observed and modeled ground temperatures prior to and immediately after the snow event. Prior to the event, the mean difference is effectively zero suggesting that the ground is responding only to the driving SAT. After the snow event the difference between observed and modeled ground temperatures is decidedly positive suggesting there is additional energy input into the ground which is not represented in the model. This switch is principally a result of direct radiant heating of the ground. Radiant heating of this kind accounts for the

Table 6. Comparison of Snow-Ground Thermal Model Results and Surface Ground Temperature Observations for Snow Events at EPO

					Event			Annual		
Snow Event[a]	Dates	Duration, days	T_{obs}, °C	$T_{calc,NS}$,[b] °C	Calculated Snow Effect, K	Model Snow Effect, K	Calculated Snow Effect, K	Model Snow Effect, K	Difference, K	Estimated Error[c]
A	2 Nov. 1994–22 Feb. 1995	112	−0.91	−2.15	1.24	1.25	0.38	0.38	0.00	0.06
B	16 Jan. 1996–16 March 1996	60	−0.11	−1.34	1.23	0.74	0.20	0.12	0.08	0.10
C	20 Jan. 1999–3 March 1999	42	−0.51	−1.66	1.15	0.86	0.13	0.10	0.03	0.04

[a]Snow event labels are given in Table 3.
[b]$T_{calc,NS}$ is the calculated mean temperature at 10 cm assuming no snow was present for the period of time associated with the labeled event.
[c]Estimated error is based on missing data from the ground temperature observations (T_{obs}) and indicates the 95% confidence interval.

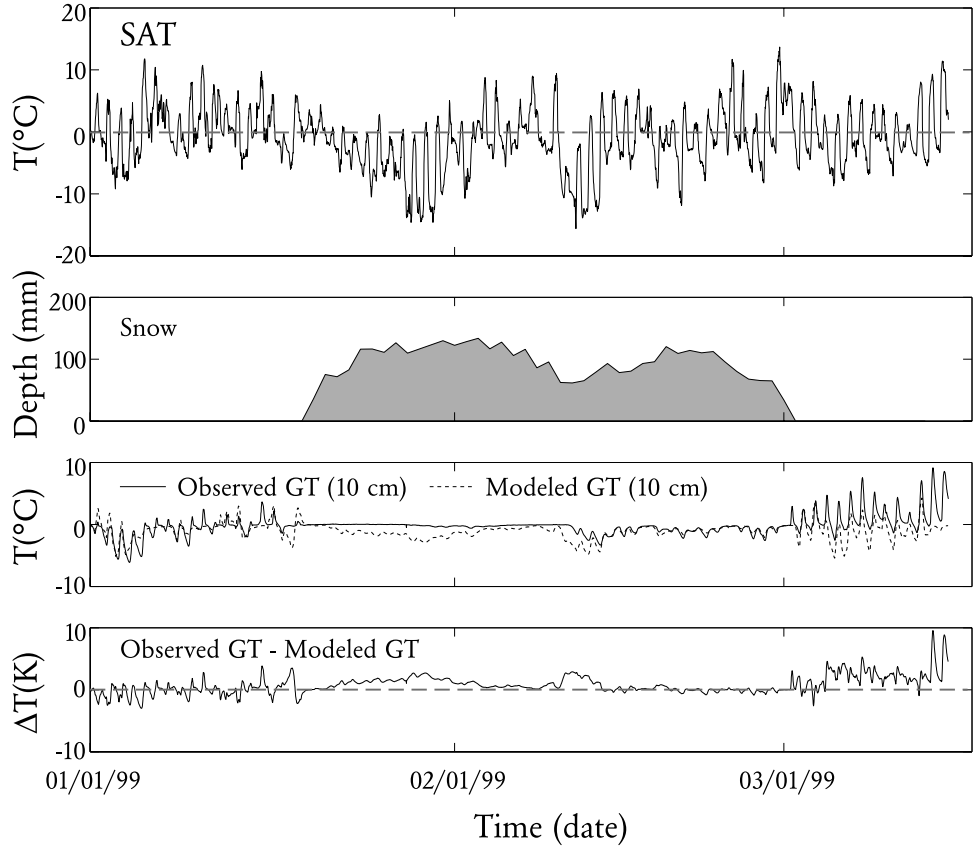

Figure 8. Influence of snow events on ground temperatures during 1999 at EPO. The SAT and snow observations are used as input into the snow-ground thermal model. Model output at 10 cm depth in the ground is compared to observed ground temperatures at 10 cm depth in the third panel. The difference between observed and modeled ground temperatures improves in mid-February likely due to a thermal compaction of the snow pack.

majority of the offset between mean annual air and ground temperatures in midlatitudes, but plays no significant role in determining ground temperatures in the presence of snow.

[41] Table 6 compares the observed influence snow has on ground temperatures at EPO and model results. The table presents observations of ground temperature at 10 cm depth for the period of time snow is present in each of the 3 years. For reference, calculated mean ground temperatures neglecting snow ($T_{calc,NS}$) are given at a depth of 10 cm. The difference between the observed and calculated temperatures gives the calculated "snow effect" for the period of time of the event. The model predicted magnitude of ground temperature change associated with each snow event for the period of time snow is on the ground is also given. The section labeled "Annual" in Table 6 presents the influence each of the events has on mean annual ground temperatures. The differences between the modeled and observed annualized snow effect and the estimated error based on missing observations are also presented.

[42] Event A has a long duration (112 days) masking the ground for much of the winter when air temperatures are less than 0°C. This insulating of the ground results in a net warming of 1.24 K over the snow event period which equates to a 0.38 K increase in the annual mean. In contrast, events B and C are late winter, relatively short-duration events that have considerable warming (1.23 K and 1.15 K, respectively) relative to air temperatures for the period of time snow is present, but produce much smaller changes (0.20 K and 0.13 K, respectively) on mean annual ground temperatures. Model results for these two events underestimate the observed snow effect but can be made to predict the observed effect more closely by adjusting the snow thermal diffusivity to a lower value (consistent with mid to late winter snow cover being less wet than snow arriving in the late fall to early winter), but such adjustments would be arbitrary. Importantly, differences between the calculated and modeled annualized snow effect are within the calculated uncertainty bounds. For all events, the model correctly predicts the sign, relative magnitude, and numeric value (to within the estimated error) of snow's influence on ground temperatures, suggesting that our relatively simple model captures the essence of the annual snow event's thermal influence on ground temperatures at EPO.

5.2. Application of Model to NWS Data

[43] In addition to data from EPO, we test the snow-ground thermal model against a broad range of stations drawn from the NWS Co-Op array. Snow's influence on ground temperatures is calculated in the same manner as described for the EPO data, above. Comparisons are then

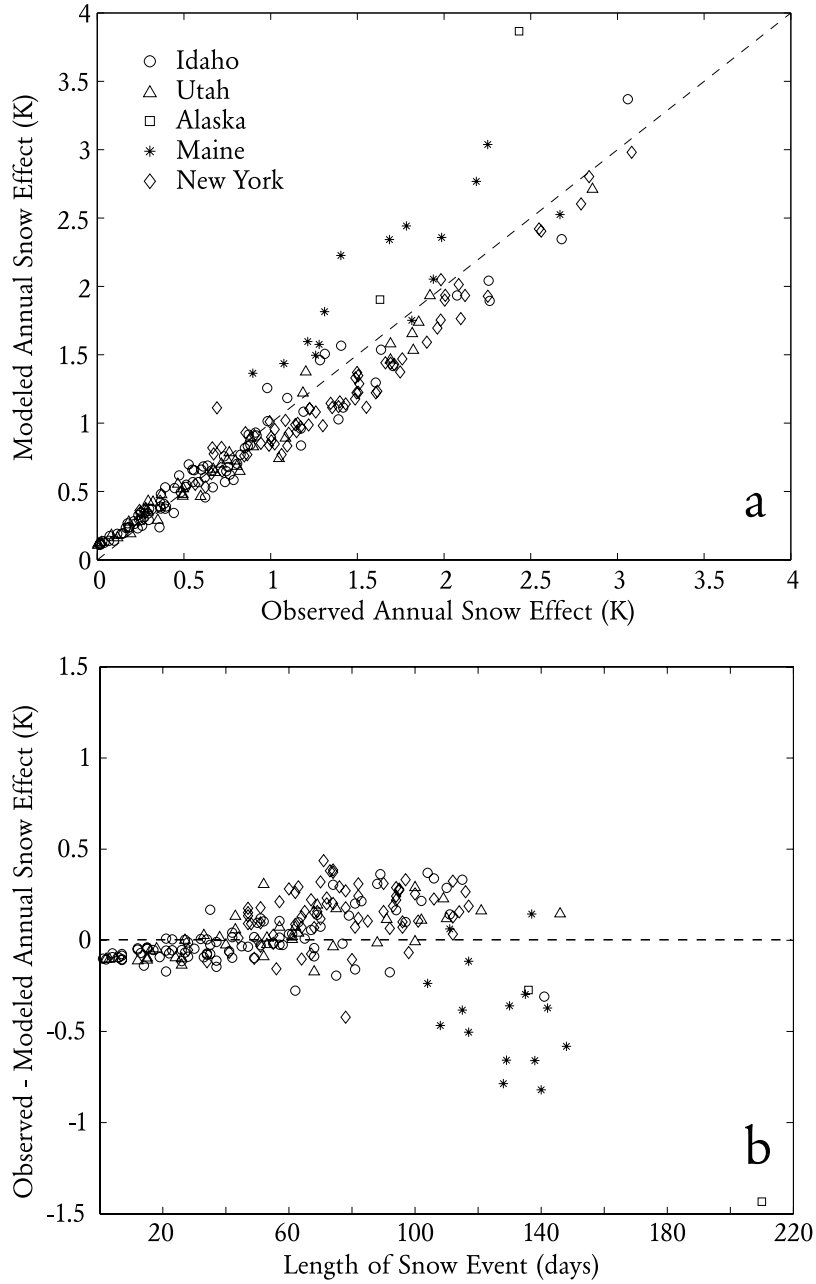

Figure 9. Comparison of modeled and observed influence of snow on mean annual ground temperatures from NWS sites in North America. (a) Comparison of observed and modeled snow effects. The dashed line indicates the one-to-one correspondence. The snow-ground thermal model performs extremely well in midlatitude areas with annual snow seasons of less than 120 days. (b) Difference between observed and modeled snow effects as a function of length of snow event. As the length of the annual snow event increases, model performance degrades.

made between the annualized modeled snow effect (the influence of snow on the mean annual SGT) and the annualized observed snow effect. Since no site specific thermal parameter information is available from the NWS sites, a common set of model parameters for the snow and ground thermal properties is employed across all NWS stations and years. These are given in Table 5.

[44] The annualized results of this test for 217 station years (Figure 9) indicates the fidelity with which the snow-ground thermal model reproduces the observed influence of snow cover on ground temperatures over a wide range of conditions. The dashed line in Figure 9a represents the one-to-one correspondence; modeled values falling on this line would "perfectly" reproduce the annualized observed mean snow effect. The correlation coefficients for the data in Figure 9a is 0.96. We also tested the time series of model and observed snow effect at individual sites within the data set. For the individual sites in the NWS data set, interannual

correlation of modeled and observed snow effect range from 0.81 to 0.99, strongly indicating that the model is capable of detecting trends in snow's influence on ground temperatures across multiple years.

[45] Figure 9 provides several insights into the value of the relatively simple snow-ground thermal model. First, while snow can either warm or cool the ground depending on its timing and duration (as pointed out in the section on sensitivity), Figure 9a indicates that at these sites and across the years of record in the NWS data set snow cover always warms the mean annual SGT.

[46] Second, the modeled snow effect predicts the observed snow effect extremely well. For station years with a modeled snow effect of less than 1 K (Figure 9a), the RMS difference between model predictions and observations is 0.10 K. The model still functions moderately well under more severe winter conditions, where the annualized snow effect may be as large as 3 K, but the scatter between model results and observations becomes greater as the snow effect becomes larger. The RMS difference between model and observations for all events with a modeled snow effect of greater than 1 K is 0.27 K.

[47] Third, Figure 9b suggests that the scatter is correlated with the length of time snow is on the ground. In general the model performs extremely well in areas where snow seasons are shorter than 60 days and moderately well where snow seasons are between 60 and 100 days. The large scatter for events greater than 120 days results primarily from stations in Maine. This degradation of model results is likely due to the temporal evolution of the snow thermal parameters and the increased period of time that melt dynamics influence ground temperatures, concessions that are made in favor of the ability to apply the model as broadly as possible. Though neither of these aspects of snow physics is currently incorporated into the snow-ground thermal model, both could be included in future versions of the model with the associated need for additional a priori information.

[48] Finally, ground temperatures from the stations in Alaska (the most northerly stations of those in the data set and the stations with the longest snow season) are reproduced relatively poorly by the model. This is almost certainly due to the fact that the snow at these particular sites overlies permafrost, the dynamics of which are not incorporated in the model.

6. Discussion

[49] This modeling study offers insight into how variations in seasonal snow cover influence the mean annual SGT-SAT difference. In this sensitivity and calibration study we have focused on differences between the magnitude of air and ground temperatures over an annual cycle. An objective in developing this model is to evaluate long-term changes in the offset between air and ground temperatures due to snow cover. Snow may degrade the coupling between air and ground temperature (this coupling is an important assumption in the use of borehole temperature-depth profiles to reconstruct surface temperature variations) if it introduces long-term systematic changes in the temperature difference.

[50] Midlatitude continental areas in the Northern Hemisphere indicate greatest recent (1976 to 2000) warming during the winter months [*Jones et al.*, 2000]. If snow insulates the ground during this warming, ground temperatures may not record the full magnitude of warming. However, as we have shown the details of differences between air and ground temperatures depend on when the snow comes, how long it stays, and its depth. Recent work on snow cover variability and long-term trends suggest that in Northern Hemisphere midlatitude areas the most significant change in the snow season is that it is ending sooner [*Groisman et al.*, 1994; *Frei and Robinson*, 1999; *Frei et al.*, 1999; *Brown*, 2000]. Figure 5 indicates that the effect of shorter snow duration with other aspects generally being the same leads to apparent ground warming relative to SAT trends. The net effect of these two hemispheric effects on ground temperature (SAT warming in the presence during winter and shorter snow duration) may lead to offsetting changes in SGT.

[51] The model presented here contains obvious simplifications of the physics of snow and the nature of the snow year. In our model, snow is represented as a layer that varies in depth with time. However, the thermal properties of snow are assumed to be homogeneous in both space and time. Actual snow undergoes compaction due to melting and refreezing, effectively changing the density and thermal parameters of the medium as a function of time. In addition, snow tends to stratify with denser layers near the bottom of the snow column. Snow melt percolates through the snow pack and provides a mechanism by which some thermal communication between the surface of the snow pack and the ground surface can take place, though in most areas this process is limited in its temporal duration. Our model could be modified to account for these and other complexities of snow pack evolution, but this would require a much larger set of input parameters effectively negating the utility of our model's simplicity. The power of a model based primarily on onset and duration of the snow season is the availability of these parameters from global satellite and meteorological observations. These data can then be used to compute the effect of snow cover on ground temperatures used to infer climatic change over the length of the observational record.

[52] It should also be noted that the model presented here is designed to understand the seasonal and annual variations in SGT due to transient snow cover. The answer to the question of whether snow can be viewed as a conductive insulator or a highly nonlinear moderator of ground temperatures is largely a function of the time frame of interest. As demonstrated in Figure 9, over large spatial areas the first-order effect of snow on the annual mean SGT is that of a simple insulator. However, the value of this approach decreases as one examines increasingly finer timescales.

[53] A caveat of this snow-ground thermal model is that we assume that energy transfer across the ground-air interface is via conductive heat transfer. We note however, that for borehole temperature depth profiles to be properly interpreted in terms of SGT change, the thermal regime must be conductive and efforts are made by the borehole community to ensure that the temperature-depth records they utilize in reconstructions are governed by conductive heat transfer. Therefore we feel that this snow-ground thermal model can safely be applied to understand the

influence of snow cover on ground temperatures and temperature-depth profiles that are interpreted in terms of a changing SGT.

7. Conclusions

[54] On the basis of our efforts to model the influence of seasonal snow cover on mean annual ground temperatures, we draw the following conclusions:

[55] 1. The influence of snow cover on the mean annual SGT can be effectively modeled via a simple, two-layered, forward finite difference approximation. Such a model can be readily applied to available meteorological observations over much of the globe.

[56] 2. Modeling of snow cover indicates that for a given set of thermal parameters and surface temperature driving functions there is a critical thickness of snow cover, beyond which all diurnal and seasonal temperature fluctuations are damped prior to reaching the ground. For the set of snow thermal parameters and driving functions presented here, this thickness is about 1 m. Lesser snow thicknesses must be modeled individually.

[57] 3. Onset time and duration of the snow event have a significant, nonlinear influence on the mean annual SGT. The magnitude of that influence also depends on the SAT in the region. Details of the accumulation and ablation of snow are considerably less important than onset time and duration.

[58] 4. Snow cover can produce either warming or cooling of the SGT relative to the SAT. Model results simulating conditions in northwestern Utah indicate that the influence of snow cover on the mean annual SGT ranges from −1.0 K to +1 K for snow depths of 1 m. A phase diagram/nomogram showing the quantitative snow effect on SGT can be developed for any location and is a useful tool to investigate possible changes in the snow effect over time.

[59] 5. Ground temperatures over three winter seasons in which snow was present at EPO in northwestern Utah were simulated using actual SAT and snow depths as model inputs. Including snow in the model significantly reduced differences between predicted and observed ground temperatures to values within the observational uncertainties.

[60] 6. Application of the snow-ground thermal model to 217 station years of data from NWS sites across North America suggests that a simple conductive model with appropriate information on site specific conditions (snow pack thermal parameters) can effectively predict the observed influence snow cover has on annual mean SGT.

[61] These conclusions indicate that variation in seasonal snow cover can be an important factor in the interpretation of borehole temperature records for regional climate change in the midlatitudes. With a verified, practical snow-ground thermal model established, we can now address critical climate change questions. How would possibly changing snow conditions through time at a specific site affect the tracking of ground and air temperatures at timescales relevant to climate change studies? Additionally, how much of the 20th century warming in extratropical continental regions inferred from borehole temperature studies (in contrast to SAT or proxy-based studies) can be attributed to snow's influence on ground temperatures?

[62] **Acknowledgments.** We would like to thank the many colleagues who have offered their advice and support of this work. The paper benefited immensely from the review and comments of many; in particular, the conversations with and comments from Matthew Sturm and Tad Pfeffer were instrumental to the final form of the paper. This work was supported by the National Science Foundation under NSF grant EAR-0126029.

References

Abu-Hamdeh, N. H., and R. C. Reeder (2000), Soil thermal conductivity: Effects of density, moisture, salt concentration and organic matter, *Soil Sci. Soc. Am. J.*, *64*, 1285–1290.

Bartlett, M. G. (2001), Snow and the ground temperature record of climate change, M.S. thesis, Univ. of Utah, Salt Lake City.

Beltrami, H. (2002), Climate from borehole data: Energy fluxes and temperatures since 1500, *Geophys. Res. Lett.*, *29*(23), 2111, doi:10.1029/2002GL015702.

Brown, R. (2000), Northern Hemisphere snow cover variability and change, 1915–97, *J. Clim.*, *13*, 2339–2355.

Chapman, D. S., and R. N. Harris (1993), Repeat temperature measurements in borehole GC-1, northwestern Utah: Towards isolating a climate-change signal in borehole temperature profiles, *Geophys. Res. Lett.*, *20*, 1891–1894.

Essery, R., and Z. L. Yang (2001), An overview of models participating in the snow model inter-comparison project (SnowMIP), report, 8th Sci. Assem. of IAMAS, Innsbruck, Austria.

Frei, A., and D. A. Robinson (1999), Northern Hemisphere snow extent: Regional variability 1972–1994, *Int. J. Climatol.*, *19*, 1535–1560.

Frei, A., D. A. Robinson, and M. G. Hughes (1999), North American snow extent: 1900–1994, *Int. J. Climatol.*, *19*, 1517–1534.

Goodrich, L. E. (1978), Efficient numerical techniques for one-dimensional thermal problems with phase change, *Int. J. Heat Mass Transfer*, *21*, 615–621.

Goodrich, L. E. (1982), The influence of snow cover on the ground thermal regime, *Can. Geotech. J.*, *19*, 421–432.

Groisman, P. Y., T. R. Karl, R. W. Knight, and G. L. Stenchikov (1994), Changes in snow cover, temperature, and radiative heat balance over the Northern Hemisphere, *J. Clim.*, *7*, 1633–1656.

Harris, R. N., and D. S. Chapman (1995), Climate change on the Colorado Plateau of eastern Utah inferred from borehole temperatures, *J. Geophys. Res.*, *100*, 6367–6381.

Harris, R. N., and D. S. Chapman (2001), Mid-latitude (30°–60°N) climatic warming inferred by combining borehole temperatures with surface air temperatures, *Geophys. Res. Lett.*, *28*, 747–750.

Huang, S., H. N. Pollack, and P.-Y. Shen (2000), Temperature trends over the last five centuries reconstructed from borehole temperatures, *Nature*, *403*, 756–758.

Jones, P. D., M. New, D. E. Parker, S. Martin, and I. G. Rigor (2000), Surface air temperature and its changes over the past 150 years, *Rev. Geophys.*, *37*, 173–199.

Lachenbruch, A. H., and B. V. Marshall (1986), Changing climate: Geothermal evidence from permafrost in the Alaskan Arctic, *Science*, *234*, 689–696.

Pollack, H., and D. S. Chapman (1993), Underground records of changing climate, *Sci. Am.*, *268*, 44–50.

Pollack, H., and S. Huang (2000), Climate reconstruction from subsurface temperatures, *Annu. Rev. Earth Planet. Sci.*, *28*, 339–365.

Powell, W. G., et al. (1988), Continental heat flow density, in *Handbook of Terrestrial Heat-Flow Density Determination: Guidelines and Recommendations of the International Heat Flow Commission*, edited by R. Haenel, L. Rybach, and L. Stegena, pp. 167–218, Kluwer Acad., Norwell, Mass.

Press, W. H., et al. (1992), *Numerical Recipes in FORTRAN 77: The Art of Scientific Computing*, Cambridge Univ. Press, New York.

Putnam, S. N., and D. S. Chapman (1996), A geothermal climate change observatory: First year results from Emigrant Pass in northwest Utah, *J. Geophys. Res.*, *101*, 21,877–21,890.

Sturm, M., J. Holmgren, M. König, and K. Morris (1997), The thermal conductivity of seasonal snow, *J. Glaciol.*, *43*, 26–41.

Yao, M., and A. Chait (1993), An alternative formulation of the apparent heat capacity method for phase-change problems, *Numer. Heat Transfer*, *24*, 279–300.

Yen, Y. C. (1981), Review of thermal properties of snow, ice and water, *Rep. 81-10*, Cold Reg. Res. and Eng. Lab., Hanover, N. H.

M. G. Bartlett, D. S. Chapman, and R. N. Harris, Department of Geology and Geophysics, University of Utah, 135 South 1460 East WBB 719, Salt Lake City, UT 84112, USA. (bartlett@mines.utah.edu; dchapman@park.admin.utah.edu; rnharris@mines.utah.edu)